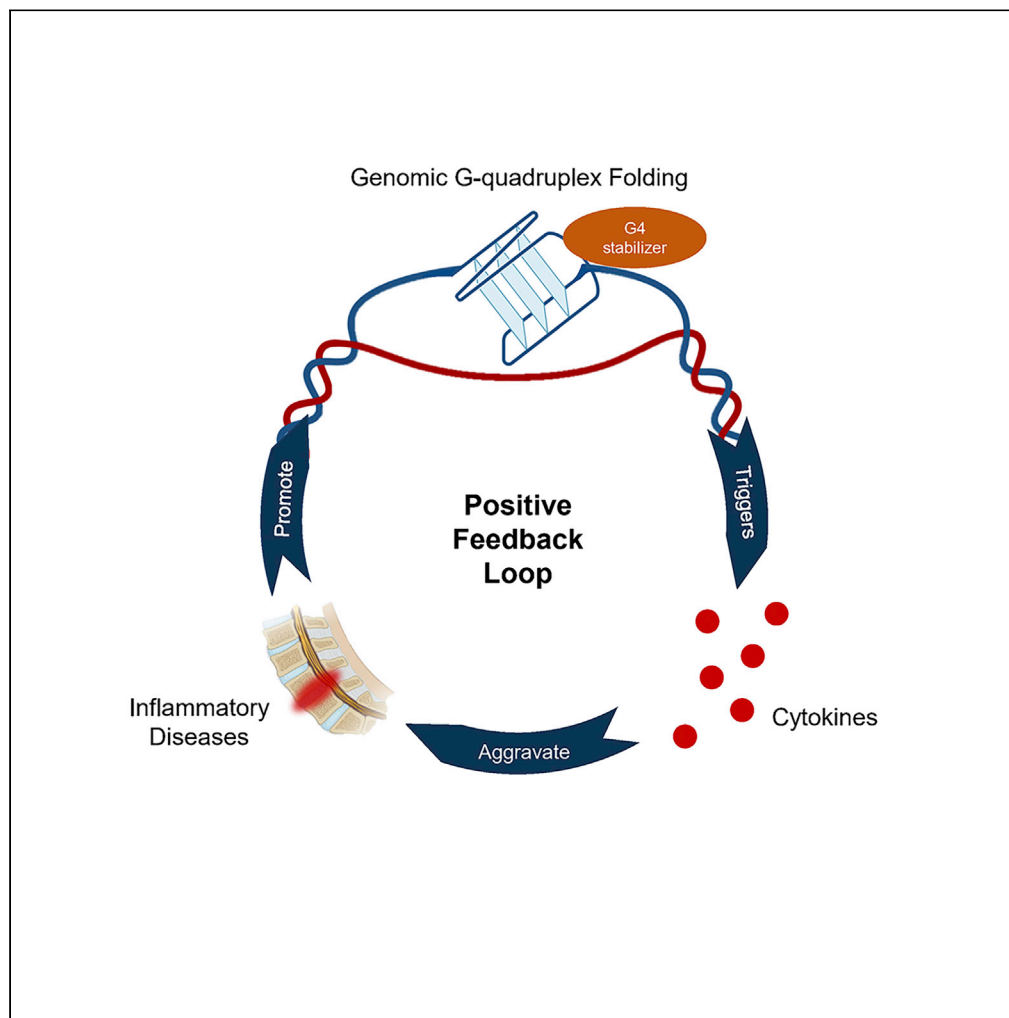


## Article

## Genomic G-quadruplex folding triggers a cytokine-mediated inflammatory feedback loop to aggravate inflammatory diseases



Xiaolin Wang,  
Shunlun Chen,  
Zhuoyang Zhao,  
..., Yanxin Luo,  
Huichuan Yu,  
Jianru Wang

yuhch5@mail.sysu.edu.cn  
(H.Y.)  
wangjru@mail.sysu.edu.cn  
(J.W.)

**Highlights**

G4-regulating genes are involved in the inflammation process

Inflammation and apoptosis triggered by G4 folding is a hallmark of disc degeneration

Inflammatory cytokines facilitate the genome-wide G4 folding

Crosstalk between G4 and inflammation provides new therapeutics for human diseases

Wang et al., iScience 25,  
105312  
November 18, 2022 © 2022  
The Authors.  
<https://doi.org/10.1016/j.isci.2022.105312>

## Article

## Genomic G-quadruplex folding triggers a cytokine-mediated inflammatory feedback loop to aggravate inflammatory diseases

Xiaolin Wang,<sup>1,2,3,5</sup> Shunlun Chen,<sup>1,2,4,5</sup> Zhuoyang Zhao,<sup>1,2,4</sup> Fan Chen,<sup>4</sup> Yuming Huang,<sup>4</sup> Xingyu Guo,<sup>4</sup> Linchuan Lei,<sup>4</sup> Wantao Wang,<sup>4</sup> Yanxin Luo,<sup>1,2,3</sup> Huichuan Yu,<sup>1,2,3,\*</sup> and Jianru Wang<sup>4,6,\*</sup>

## SUMMARY

**DNA G-quadruplex is a non-canonical secondary structure that could epigenetically regulate gene expression. To investigate the regulating role of G-quadruplex, we devised an integrating method to perform the algorithm profiling and genome-wide analysis for the dynamic change of genomic G-quadruplex and RNA profiles in rat nucleus pulposus cells by inducing G-quadruplex folding with multiple stabilizers. A group of genes potentially regulated by G-quadruplex and involved in the inflammation process has been identified. We found that G-quadruplex folding triggers inflammation response by upregulating inflammatory cytokines, which could promote G-quadruplex folding in a manner of positive feedback loop. Moreover, we confirmed that G-quadruplex is a marker indicating elevated inflammatory status and G-quadruplex folding facilitates the development of inflammatory diseases using *in vivo* intervertebral disc degeneration models. The crosstalk between G-quadruplex and inflammatory cytokines plays a vital role in regulating inflammation-derived diseases, which may provide new insights into the blocking target.**

## INTRODUCTION

Inflammation is a defense mechanism that protects higher organisms from infection and injury, whereas aberrant and uncontrolled inflammation triggers multiple diseases (Feehan and Gilroy, 2019; Medzhitov, 2008; Strowig et al., 2012). Because of the similar inflammation-dependent nature, inflammation has played a vital role in inflammatory conditions such as cancer, severe COVID-19, Alzheimer's disease, cardiovascular disease, and osteoarthritis (Crusz and Balkwill, 2015; Feehan and Gilroy, 2019; Sun et al., 2022). The inflammatory cytokines such as TNF- $\alpha$ , IL-6, and IL-1 $\beta$  have been shown to play a key role in multiple diseases by regulating inflammatory response, including cancers, chronic liver disease, Parkinson's disease, and intervertebral disc degeneration (IVDD) (Carelli et al., 2018; Cubero et al., 2019; Risbud and Shapiro, 2014; Wang et al., 2020).

It has been demonstrated that the inflammatory cytokines could be regulated by multiple epigenetic mechanisms, such as the genomic secondary structure and modification and transcription factor-targeting regulation (Markopoulos et al., 2019; Tarnowski et al., 2021). DNA G-Quadruplex (G4) is a non-canonical four-stranded secondary structure that may appear in guanine-rich nucleotide sequences (Sen and Gilbert, 1988; Kwok and Merrick, 2017). A potential G4 sequence (PQS) is featured by two or more G-tetrads (Hoogsteen hydrogen bonding of four guanines) stacked on top of each other (Sen and Gilbert, 1988; Lane et al., 2008). PQS is abundant in the genome of humans, chimpanzees, mice, rats, bacteria, etc (Marsico et al., 2019; Sengupta et al., 2021), and it is enriched in gene promoters and telomeres. G4 has been visualized and detected in the human and rat genomic region with PQS by using chemical and immunological methods (Hansel-Hertsch et al., 2018; Varshney et al., 2020). Moreover, G4 has been recognized to play an important role in multiple key biological processes that involve replication, transcription, translation, genome instability, and telomere maintenance across multiple species (Verma et al., 2008; Kwok and Merrick, 2017; Sengupta et al., 2021). In transcription regulation, G4 was found to facilitate the adherence of transcription initiation complex, increase promoter-proximal Pol II pausing, control CpG island methylation and interact with transcription factors (Lago et al., 2021; Li et al., 2021; Lyu et al., 2021; Mao et al., 2018). Huang et al. demonstrated that custom-made small molecule compounds could act with DNA to

<sup>1</sup>Guangdong Provincial Key Laboratory of Colorectal and Pelvic Floor Diseases, The Sixth Affiliated Hospital, Sun Yat-sen University, Guangzhou, Guangdong, China

<sup>2</sup>Guangdong Institute of Gastroenterology, Guangzhou, Guangdong, China

<sup>3</sup>Department of Colorectal Surgery, The Sixth Affiliated Hospital, Sun Yat-sen University, Guangzhou, Guangdong, China

<sup>4</sup>Department of Spine Surgery, Guangdong Provincial Key Laboratory of Orthopaedics and Traumatology, The First Affiliated Hospital of Sun Yat-sen University, Guangzhou 510080, China

<sup>5</sup>These authors contributed equally

<sup>6</sup>Lead contact

\*Correspondence: yuhch5@mail.sysu.edu.cn (H.Y.), wangjru@mail.sysu.edu.cn (J.W.)

<https://doi.org/10.1016/j.isci.2022.105312>



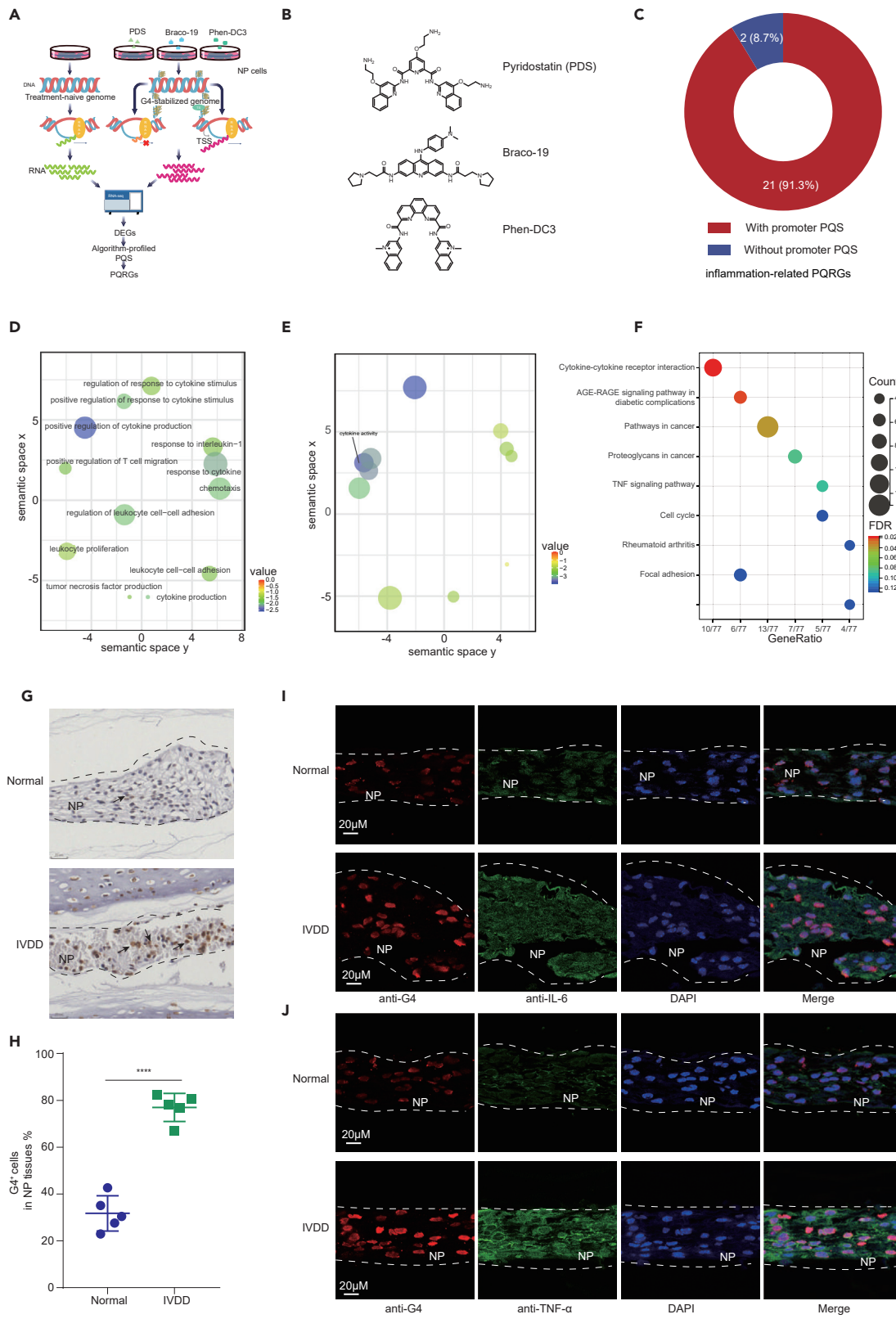


**Figure 1. G4 folding involves in the gene regulation of inflammation process and disease**

(A) Workflow of the method we devised to identify the PQRGs.

(B) The chemical structure of PDS, Braco-19, and Phen-DC3.

(C) Pie chart of potential G4-regulating inflammation-related genes with or without in promoter PQS.

(D and E) GO enrichment analysis of identified PQRGs, and the analyses regarding the terms related to biological process and molecular function were shown.

(F) KEGG pathway enrichment analysis of identified PQRGs.

(G and H) Representative images and quantitative analysis of immunohistochemistry assay for genomic G4 in the intervertebral discs of IVDD mice models. Scale bars, 50  $\mu$ M.

(I and J) Representative images of immunofluorescence assay for expression and co-localization of folded G4, TNF- $\alpha$ , and IL-6 in the intervertebral discs of IVDD mice models. Scale bars, 20  $\mu$ M.

G4, G-Quadrupelex; PQRG, potential G4-regulating gene; DEG, differentially expressed genes; PQS, potential G4 sequence; TSS, the transcription start site; IVDD, intervertebral disc degeneration; NP, nucleus pulposus. Data are expressed as mean  $\pm$  SEM (n = 5); \*p < 0.05, \*\*p < 0.01, \*\*\*p < 0.001, \*\*\*\*p < 0.0001, compared to the control group.

stabilize G4 with multiple conformations in different PQS that may participate in the epigenetic regulation of mammal genes, but the validation with *in vitro* and *in vivo* models is lacking (Huang et al., 2009; Liu et al., 2021).

In this study, we devised a method to identify the potential G4-regulating genes (PQRGs) by integrating the genomic PQS profiled by the algorithm and differentially expressed genes (DEGs) after stabilizing genomic G4. By using this method in the inflammatory disease models, we identified a group of PQRGs that were associated with the inflammation process. In addition, we found that PQS was abundant in the genes expressing inflammation cytokines. Therefore, we speculated that the genomic G4 folding may play a vital role in inflammation-derived diseases by regulating the expression of inflammatory cytokines. Based on our findings, the crosstalk between the genomic G4 folding and the inflammation process was proposed. We demonstrated that the crosstalk plays a vital role in regulating the development of inflammatory diseases using *in vivo* animal models, which may provide new insights into the understanding of inflammatory diseases and the development of blocking targets for the therapeutics.

**RESULTS****Genome-wide analysis identifies the potential G4-regulating genes that involve in the inflammation process**

To decipher the roles of G4 in inflammation regulation, we predefined a group of PQRGs that are subjected to the regulation of G4 folding. We devised a method to identify PQRGs by integrating the algorithm-profiled PQS and G4 stabilization-specific DEGs. The transcriptome profiling was performed in rat NP cells with the naive or stabilized status of genomic G4 to identify the DEGs (Figure 1A). The stabilizers, including Pyridostatin (PDS), Braco-19, and Phen-DC3, were used to stabilize the genomic G4 (Figure 1B). As a result, we identified 653 DEGs that were subject to genomic G4 stabilization. After the genes with absent PQS were filtered, a total of 163 PQRGs were identified. Next, we computationally investigated PQS in the promoter of inflammation-related PQRGs. We found that 91.3% of the gene promoters contained sequences with a high propensity to form G4s (Figures 1C, Table S1 and S2).

Based on the Gene Ontology (GO) analysis of the PQRGs, we found that G4 folding was involved in the inflammation process, particularly in the inflammatory response regulation, cytokine production involved in immune response, and cytokine activity (Figures 1D, 1E, Tables S3 and S4). Moreover, we found that G4 folding regulated the genes involve in cytokine-cytokine receptor interaction according to the Kyoto Encyclopedia of Genes and Genomes (KEGG) analysis of PQRGs (Figures 1F, Tables S5 and S6).

To verify these findings, we visualized the *in vivo* association of G4 folding and inflammatory response triggered by cytokines with immunofluorescent and immunohistochemical assays in IVDD animal models. As a result, more folded G4 was found in the IVDD group with elevated TNF- $\alpha$  and IL-6 expression compared with the control group (Figures 1G–1J). Taken together, G4 folding may participate in the regulation of the inflammatory process, and it is a marker of elevated inflammatory status.

**G4 stabilization upregulates inflammatory cytokines**

To investigate the regulatory role of G4 folding in the expression of inflammatory cytokines, we treated the NP cells with PDS, Braco-19, and Phen-DC3, respectively, to facilitate genomic G4 stabilization. We found

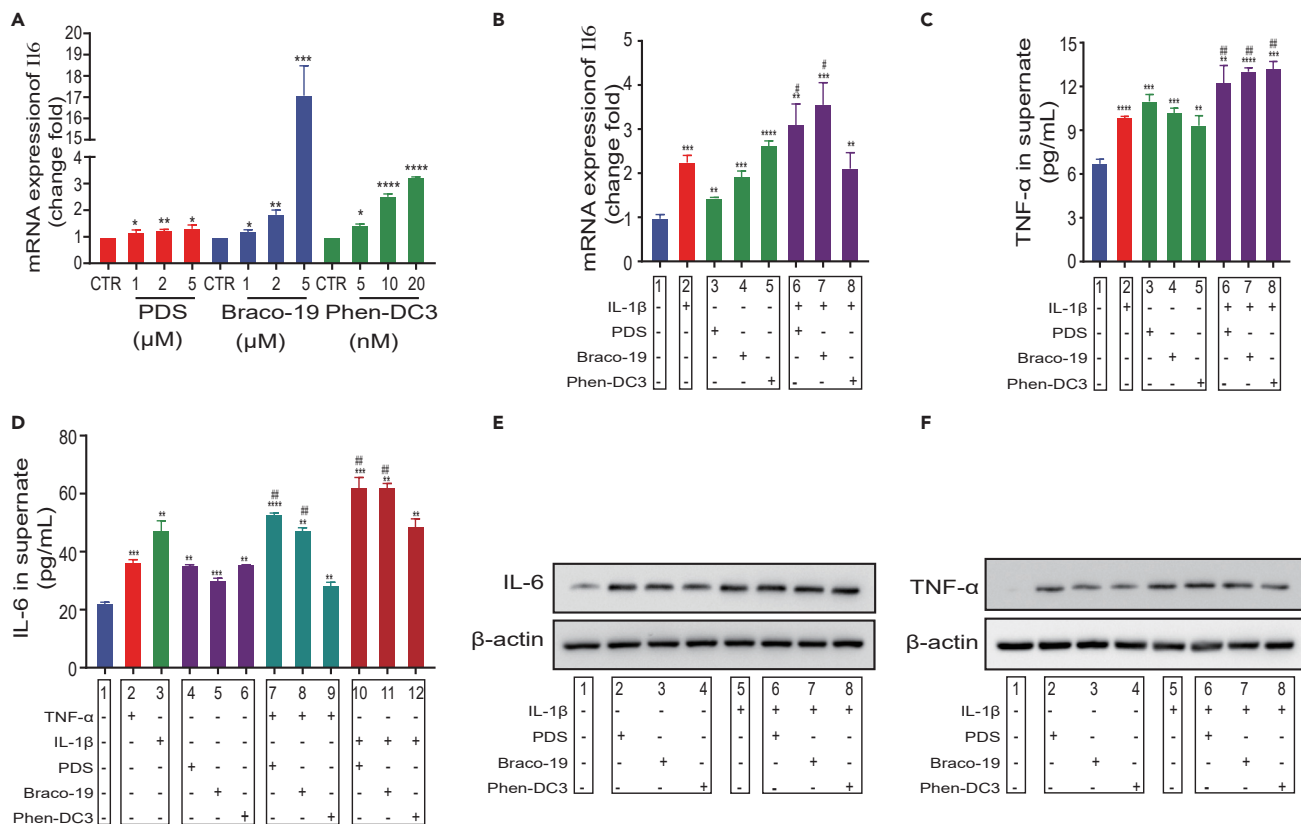


**Figure 2. G4 stabilization induces an inflammation response by upregulating inflammatory cytokine**

(A and B) mRNA expression of IL6 after the single or combined treatment of PDS, Braco-19, Phen-DC3 and IL-1β (10 ng/mL).

(C–F) ELISA and western blot assays for the expression of IL-6 and TNF-α after the single or combined treatment of PDS, Braco-19, Phen-DC3, TNF-α (20 ng/mL) and IL-1β (10 ng/mL).

G4, G-Quadruplex; NP, nucleus pulposus; CTR, control. Data are expressed as mean ± SEM (n = 3); \*p < 0.05, \*\*p < 0.01, \*\*\*p < 0.001, \*\*\*\*p < 0.0001, compared to the control group. #p < 0.05, ##p < 0.01, ###p < 0.001, ####p < 0.0001, compared to the TNF-α or IL-1β group.

that G4 stabilization could promote mRNA expression of IL6 in NP cells in a dose-dependent manner (Figure 2 A, B). Of interest, G4 stabilization could further increase the expression of multiple inflammatory cytokines following the treatment of TNF-α or IL-1β, indicating that the inflammation process could be aggravated by the potential crosstalk between inflammatory cytokines and G4 folding in inflammation-related genes. Finally, we conducted ELISA and Western blot assays to verify that the upregulated protein expression subjected to G4 folding was consistent with the mRNA expression change (Figures 2C–2F).

### Inflammatory cytokines facilitate genomic G4 stabilization

To explore the role of inflammatory cytokines in G4 folding, NP cells were incubated for 24h with TNF-α, IL-1β, and IL-6 ranging from 10–100 ng/mL, respectively. Immunological assays with anti-G4 antibodies were used to detect the genomic G4 folding. In the immunofluorescence assay, folded G4 increased gradually from the treatment of inflammatory cytokines at 10 ng/mL and exhibited a dramatic increase at 100 ng/mL (Figure 3A). Furthermore, more folded G4 was found in the groups treated by TNF-α, IL-1β, or IL-6 combined with G4 stabilizers compared with the groups treated by TNF-α, IL-1β, or IL-6 alone (Figure 3B). The dot blot assay also confirmed that TNF-α, IL-1β, or IL-6 could promote G4 folding in a dose-dependent manner (Figures 3C–3F). In summary, inflammatory cytokines could promote genomic G4 folding in a manner of positive feedback loop.

### G4 stabilization increases apoptosis in NP cells

First, we observed that G4 stabilization achieved with PDS, Braco-19, and Phen-DC3 treatment suppressed NP cell viability in a dose-dependent manner, respectively (Figure 4A). To elucidate the mechanism

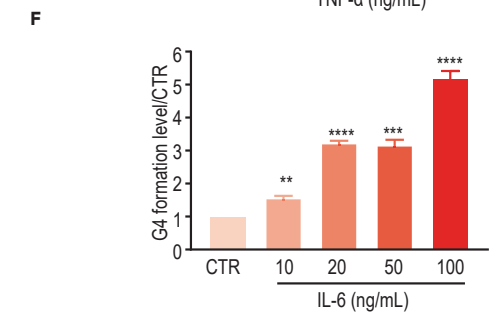
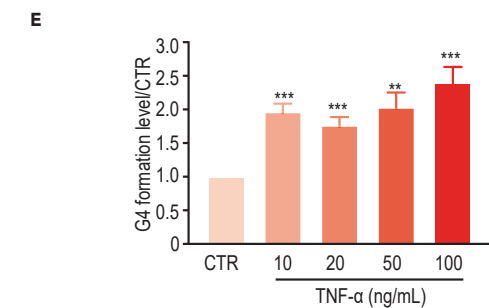
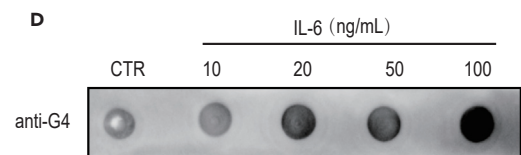
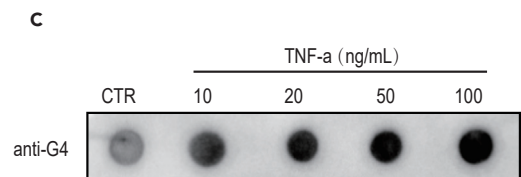
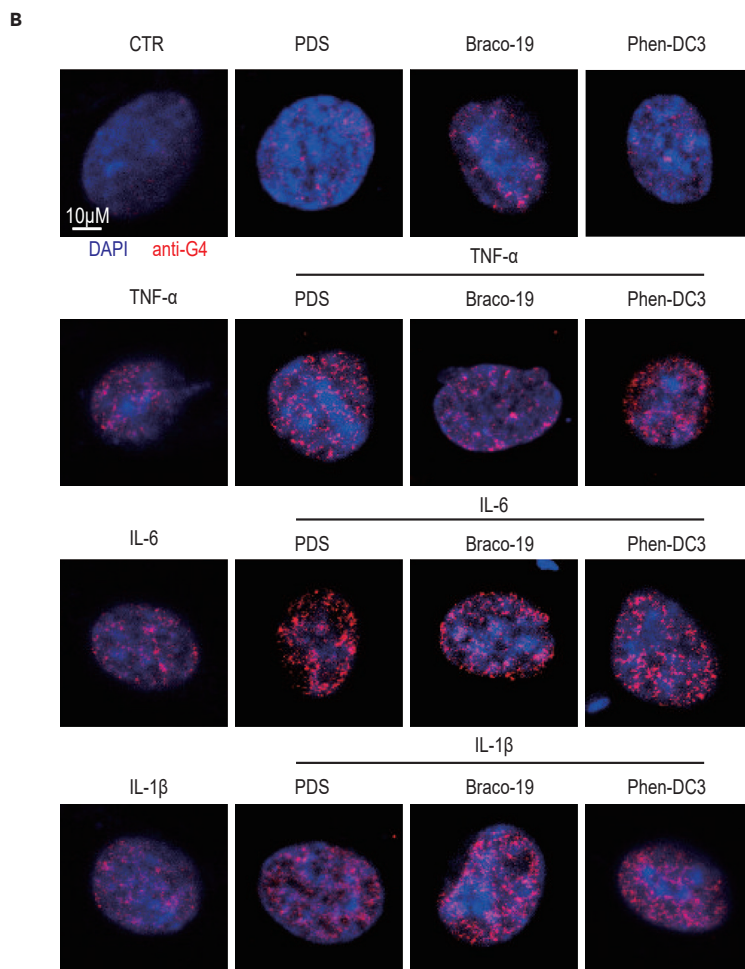
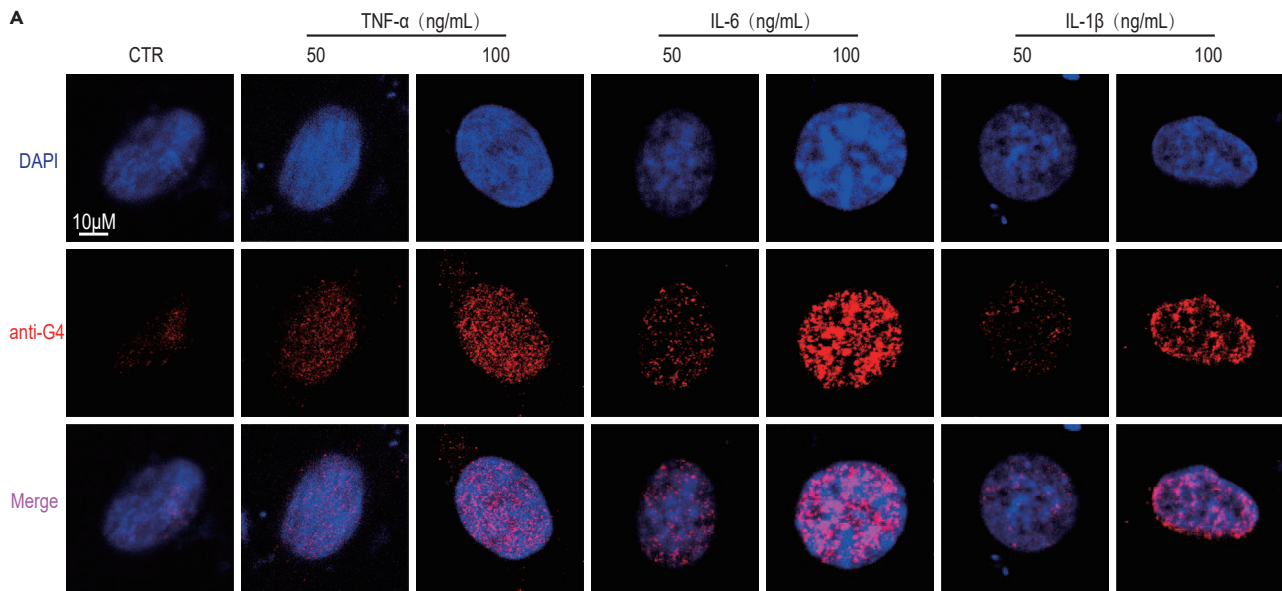




**Figure 3. Inflammatory cytokines promote G4 folding**

(A) Representative images of immunofluorescence assay for genomic G4 folding under the treatment of TNF- $\alpha$ , IL-1 $\beta$ , or IL-6. Scale bars, 10  $\mu$ M.

(B) Representative images of immunofluorescence assay for genomic G4 folding under the treatment of G4 stabilizers combined with TNF- $\alpha$ , IL-1 $\beta$ , or IL-6. Scale bars, 10  $\mu$ M.

(C–F) Dot blot assay for genomic G4 under the TNF- $\alpha$  or IL-6 treatment.

NP, nucleus pulposus; G4, G-Quadruplex; CTR, control. Data are expressed as mean  $\pm$  SEM (n = 3); \*p < 0.05, \*\*p < 0.01, \*\*\*p < 0.001, \*\*\*\*p < 0.0001, compared to the control group.

underlying the cell death after G4 stabilization, we used propidium iodide (PI) staining and Annexin V-fluorescein isothiocyanate (FITC) assay to evaluate whether G4 stabilization could induce apoptosis in NP cells. As a result, G4 stabilization increased the number of PI-positive cells. Importantly, the apoptosis rate was higher in the group treated with G4 stabilizers and cytokines (Figure 4B and 4C). Then, we found that the expression of apoptotic proteins, including cleaved caspase-3 and Bax, increased under the treatment of G4 stabilizers in a dose-dependent manner (Figures 4D–4I). Importantly, the expression of these proteins increased significantly more under the co-treatment with G4 stabilizers and inflammatory cytokines compared with the treatment of G4 stabilizers or inflammatory cytokines alone, indicating a potential synergistic effect of G4 stabilizers and inflammatory cytokines on apoptosis (Figures 4J–4L). Taken together, genomic G4 stabilization could increase apoptosis in NP cells.

**Genomic G4 stabilization aggravates the progression of IVDD *in vivo***

To investigate the role of G4 folding in the development of inflammatory diseases, we stabilized the genomic G4 in the mice's intervertebral discs and observed the *in vivo* progression of IVDD. The PBS, PDS, and Braco-19 were injected into the intervertebral discs (IVD) of mice, and IVDD mouse models were generated with the annulus fibrosus (AF) needle puncture. All mice underwent MRI scans 4 weeks after surgery, and we found the G4-stabilized groups displayed significantly lower signal intensity than the control group (Figures 5A–5C). Next, the HE staining and Safranin O-Fast Green staining of the IVD slice were performed (Figures 5E and 5F). Compared to the sham group, the G4-stabilized groups demonstrated classic histopathological features of IVDD, including the decreased amount of gelatinous NP tissue and the disturbed border between the NP and AF. The histological scores of the G4-stabilized groups treated with the PDS or Braco-19 were significantly higher compared with the control group (Figure 5D). Finally, the IHC staining and western blot assays for Collagen II, Aggrecan, and MMP-3 were conducted to investigate the extracellular matrix (ECM) remodeling of IVD. We found that the expression of Collagen II (Figure 5H and 5K) and Aggrecan (Figures 5I and 5L) were significantly decreased in the G4-stabilized groups, whereas the expression of MMP-3 was significantly increased (Figure 5G and 5J). Therefore, genomic G4 stabilization could significantly disturb the structural integrity of IVD and promote IVDD by regulating the inflammatory process. In summary, we found that genomic G4 folding plays a critical role in the progression of inflammation-derived diseases.

**DISCUSSION**

In this study, we treated NP cells with G4 stabilizers and found several genes potentially regulated by G4, and these genes were involved in the inflammation process, which was performed by an algorithm profiling and genome-wide analysis. We found that G4 folding could promote the production of inflammatory cytokines and induce apoptosis in rat NP cells. Of interest, we also revealed that inflammatory cytokines could promote G4 folding. These results were confirmed with *in vivo* experiments in a mouse IVDD model.

Inflammation, including acute and chronic phases, is involved in the pathogenesis and course of numerous diseases. Chronic inflammation was necessary for tumor development, and inflammation damaged DNA and promoted mutations that initiated cancer, such as liver, breast, bowel, urinary bladder, prostate, and others (Kay et al., 2019; Khandia and Munjal, 2020). Furthermore, damaged DNA could induce cytotoxicity and increase inflammatory response, which formed a positive feedback loop (Kay et al., 2019). Alzheimer's disease is a neurodegenerative disorder with pathological hallmarks of amyloid- $\beta$  plaques and neurofibrillary tangles in the brain, in which several studies have proved that inflammation may play an important role, and IL-1 $\beta$  and TNF- $\alpha$  displayed worse short-term memory functions in a mouse model (Holmes, 2013; Wang et al., 2021). Inflammation could also trigger chronic and multiple organ diseases, such as chronic kidney disease and nonalcoholic fatty liver disease (Steven et al., 2019). Importantly, the close crosstalk of inflammation with oxidative stress may contribute to cardiovascular diseases (Steven et al., 2019; Wenzel et al., 2017). Rheumatoid arthritis, a chronic inflammation-derived disorder, is characterized by generalized inflammation in synovial joints (Bedaiwi et al., 2021). Previous study has revealed that inflammation, especially triggered by IL-1 $\beta$  and TNF- $\alpha$ , exerts a vital

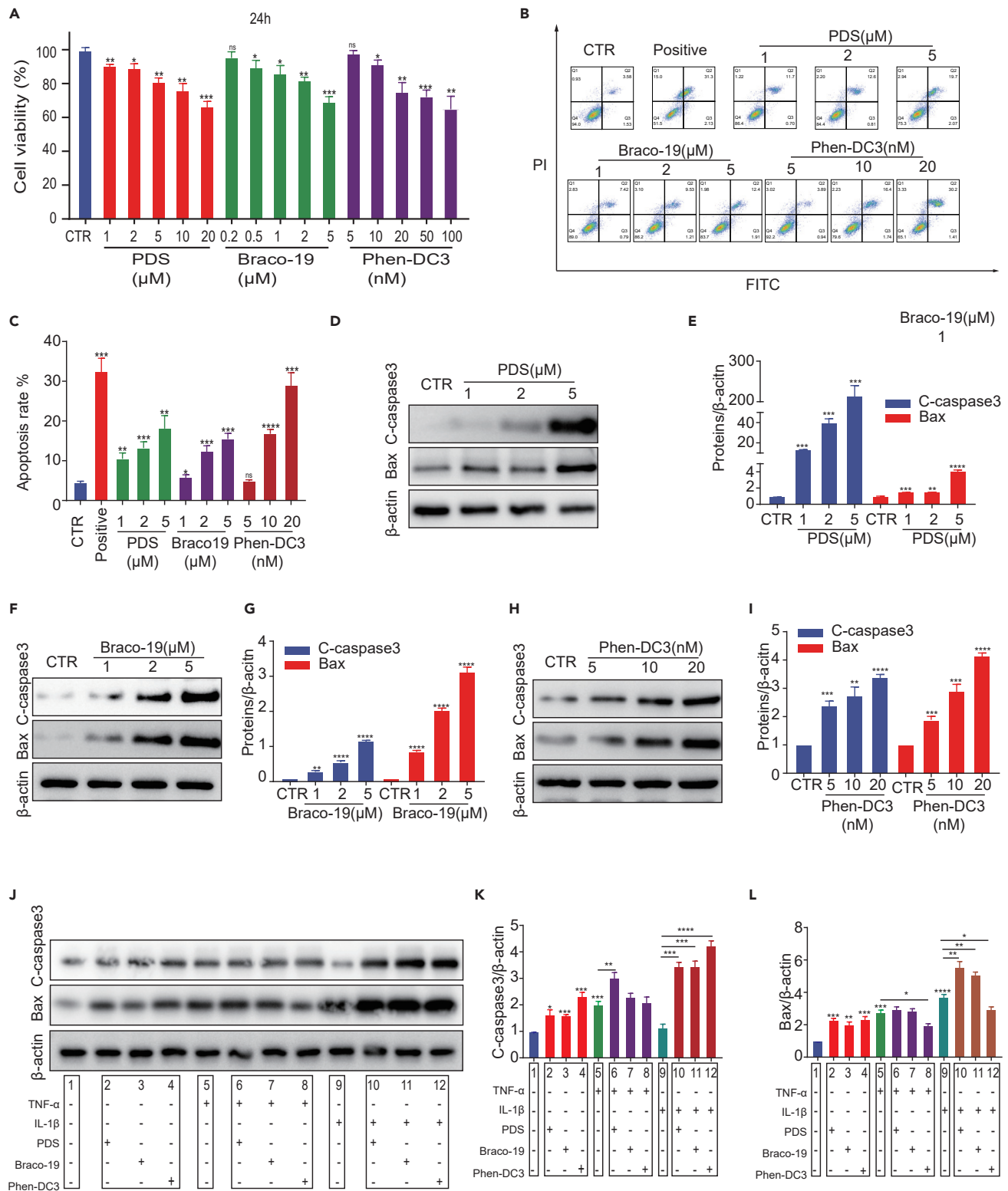




**Figure 4. Continued**

(J–L) Western blot assay for c-caspase3 and Bax under the treatment of each G4 stabilizer combined with TNF- $\alpha$  or IL-1 $\beta$ . NP, nucleus pulposus. G4 stabilizers: PDS, Braco-19, and Phen-DC3. G4, G-Quadruplex; CTR, control; PI, propidium iodide; FITC, fluorescein isothiocyanate; CCK-8, cell counting kit. Data are expressed as mean  $\pm$  SEM (n = 3); \*p < 0.05, \*\*p < 0.01, \*\*\*p < 0.001, \*\*\*\*p < 0.0001, compared to the control group.

role in the pathogenesis of osteoarthritis with cartilage loss and progressive joint degeneration (Robinson et al., 2016). In this study, we established G4-stabilized models with PDS, Braco-19, and Phen-DC3 *in vitro* and *in vivo*, and TNF- $\alpha$ , IL-1 $\beta$ , and IL-6 were used to generate cell models of inflammation and degeneration. The crosstalk between G4 and inflammatory cytokines was investigated, and the disease model of IVDD was applied to study the role of the crosstalk in inflammation-derived diseases. Considering the roles of inflammation in multiple diseases, our study may provide significant insight into the mechanism and therapeutic target of inflammation-derived disorders.

IVDD is the most common cause of low back pain that has been recognized as a global medical problem (Hartvigsen et al., 2018). The pathology of IVDD is mainly characterized by the production of inflammatory cytokines and chemokines, degeneration of the ECM consisting predominantly of type II collagen and proteoglycans, increased cell death and senescence, altered cell phenotype, and decreased NP cell abundance (Priyadarshani et al., 2016). Inflammatory response, exacerbated by inflammatory cytokines, particularly TNF- $\alpha$  and IL-1 $\beta$ , plays a key role during IVDD development (Risbud and Shapiro, 2014; Vergoesen et al., 2015; Wang et al., 2020). Previous studies have illustrated that TNF- $\alpha$  stimulation promotes IL-1 $\beta$ , IL-6, IL-8, IL-17, substance P, NO, COX-2, and PGE2 production (Koerner et al., 2016; Wang et al., 2020), whereas IL-1 $\beta$  may act as a key promoter of inflammatory cascade events by inducing IL-6, IL-8, and IL-17 production. Moreover, IL-1 $\beta$  induces CCL2/3/5/7 overexpression (Risbud and Shapiro, 2014; Wang et al., 2013). Taken together, the crosstalk we revealed between G4 and these well-characterized inflammatory cytokines further verified the importance of inflammation in driving the development of IVDD.

G4 has been proved to regulate replication, transcription, and translation, and the previous investigations predominately focused on cancer and neurological diseases (Guo and Bartel, 2016; Zimmer et al., 2016), which are inflammation-derived disorders. Recent research, using bioinformatics methods to identify PQS within promoter regions and complete gene sequences of cytokines and chemokines, find genes including IL-6, IL-12, IL-17, TNF, and TGF- $\beta$  have high PQS frequencies, particularly in their promoters (Bidula, 2021). After stabilizing G4, we found changes in genes and signaling pathways related to inflammation, immune, and apoptosis through RNA sequencing. Furthermore, we verified that G4 stabilization could upregulate TNF- $\alpha$  and IL-6, and these cytokines could promote G4 stabilization in cells. We speculate that the folded G4 may regulate the expression of inflammatory genes by the direct interaction with DNA binding proteins such as transcription factors, modulating CpG methylation and shaping chromatin to produce an inflammatory transcriptome (Lago et al., 2021; Li et al., 2021; Lyu et al., 2021; Tian et al., 2018). Therefore, we proposed that the crosstalk of G4 and inflammation may play a vital role in inflammation-derived diseases (Figure 6). Previous studies presented that the epigenetic mechanism underlying the crosstalk between molecular events participates in multiple diseases (Enuka et al., 2017), which is mechanically similar to our proposed model. Collectively, we think G4 stabilization could act as a hallmark of inflammation-derived diseases and the “G4-inflammation-G4” positive feedback loop may exert an important role in pathological processes of inflammation-derived diseases.

Here, we elucidate for the first time that the crosstalk between G4 and inflammatory cytokines plays a vital role in regulating IVDD development, which may provide new insights into the blocking target for the therapeutics of IVDD. Moreover, current studies have linked G4 formation with cancer and other human diseases. G4 stabilization could induce DNA damage and cell-cycle arrest in human breast cancer cells and reduced the viability of BRCA1/2 deficiency cancer cells (Zimmer et al., 2016). In addition, G4 regulated senescence and apoptosis of tumor cells through activating the caspases-3/7 and ATM/autophagy pathways (Beauvarlet et al., 2019; Maiti et al., 2018). Therefore, the crosstalk between G4 and inflammatory cytokines may also contribute to cancer, neurological disorders, and other inflammatory diseases, which provides therapeutic strategies and targets in the future.

**Conclusion**

This study unearthed the vital function of the crosstalk of G4 and inflammation in the progression of inflammatory diseases. We identified a group of genes that were potentially regulated by G4 and involved in the

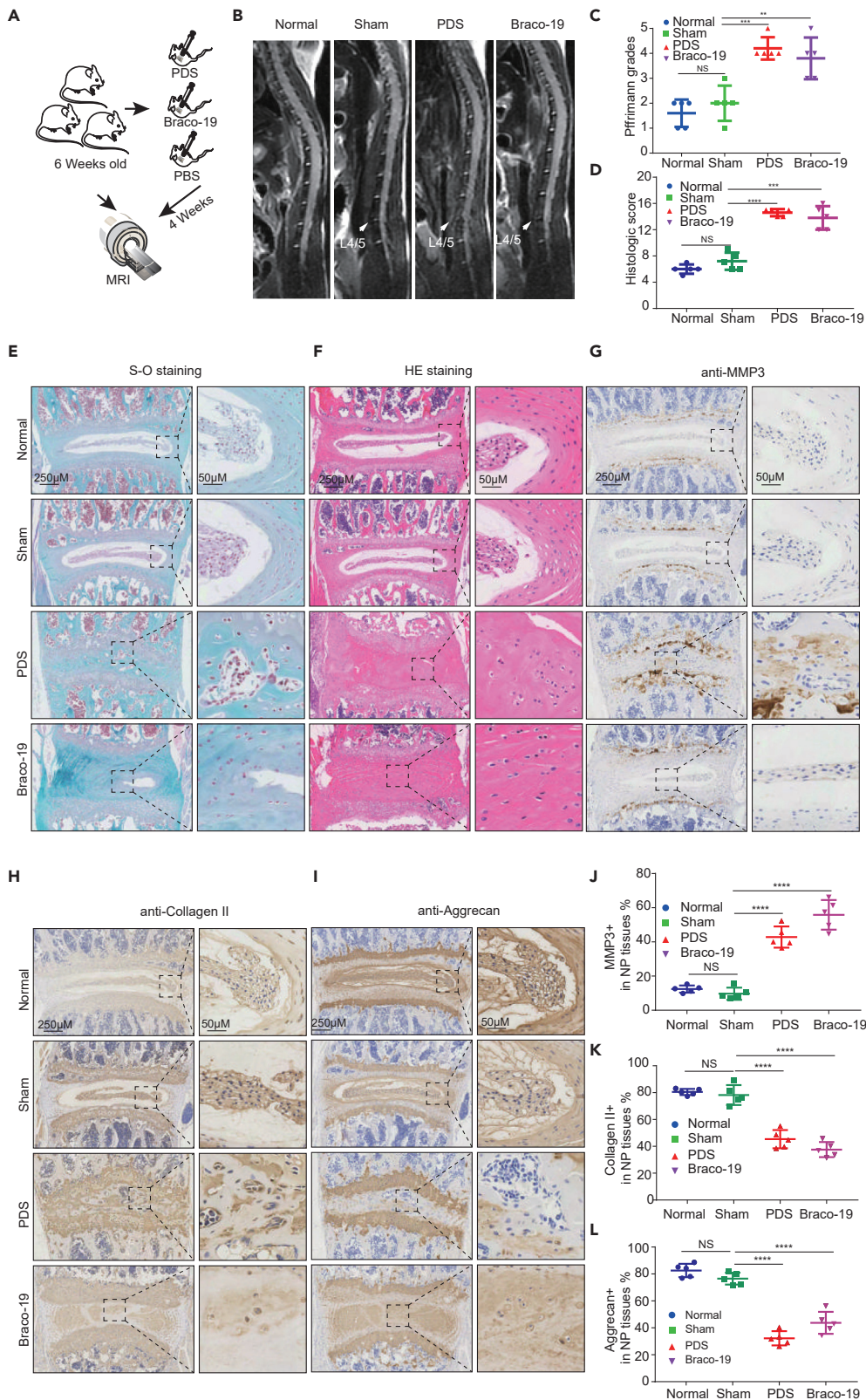


**Figure 5. Genomic G4 folding aggravates the inflammation-dependent progression of IVDD in mice**

(A and B) MRI scanning for IVDD mice models at 4 weeks after the G4 stabilizers treatment. The white arrows marked the locations of L4/L5 discs.

(C) Pfirrmann grades of MRI.

(D–F) HE staining and S-O staining of IVD with histological scores were shown. Scare bars, 250  $\mu$ M and 50  $\mu$ M.

(G and J) IHC assay for MMP3 was shown. Scare bars, 250  $\mu$ M and 50  $\mu$ M.

(H and K) IHC assay for Collagen II was shown. Scare bars, 250  $\mu$ M and 50  $\mu$ M.

(I and L) IHC assay for Aggrecan was shown. Scare bars, 250  $\mu$ M and 50  $\mu$ M.

MRI, magnetic resonance imaging; IVDD, intervertebral disc degeneration; HE, hematoxylin and eosin staining; S-O staining, Safranin O-Fast Green staining; IHC, immunohistochemistry; IVD, intervertebral disc; G4, G-Quadruplex; CTR, control. Data are expressed as mean  $\pm$  SEM (n = 5); \*p < 0.05, \*\*p < 0.01, \*\*\*p < 0.001, \*\*\*\*p < 0.0001, compared to the control group.

inflammation process. We further revealed that G4 stabilization upregulated inflammatory cytokines and apoptosis in NP cells which are well recognized as the hallmarks of disc degeneration, and inflammatory cytokines facilitate the folding of genomic G4. Therefore, the genomic fold of G4 could be recognized as a hallmark in NP cells of the degenerated disc. The crosstalk between G4 and inflammatory cytokines may provide new insights into the therapeutics for IVDD and other inflammation-derived diseases.

**Limitations of the study**

There are a few limitations in this study. We were unable to generate a patient cohort with samples to validate the G4 as a biomarker for IVDD or other inflammation diseases. It is of significance to collect patient or animal samples in a longitudinal cohort to explore the dynamic change of G4 folding and inflammation cytokines during disease development in the future. A further limitation is that the specific mechanism underlying the regulating role of genomic G4 in cytokine expression remains to be elucidated. Although we showed the systematic interaction between them in this study, it needs further investigation on each cytokine to understand how G4 and its interaction with DNA binding proteins modulate gene transcription in future studies. In addition, because of the absence of drugs for unfolding G4, we were unable to obtain the direct evidence that G4 could be served as a blocking target for IVDD treatment in animal models. However, our findings imply that the custom-made compounds and adapters that could destabilize G4 or block its interaction with DNA binding proteins may serve as a promising approach for future therapeutics.

**STAR★METHODS**

Detailed methods are provided in the online version of this paper and include the following:

- **KEY RESOURCES TABLE**
- **RESOURCE AVAILABILITY**
  - Lead contact
  - Materials availability
  - Data and code availability
- **EXPERIMENTAL MODEL AND SUBJECT DETAILS**
  - Isolation and culture of primary rat NP cells
  - Animal model and MRI
  - Ethical approval
- **METHOD DETAILS**
  - RNA-seq analysis for potential G4-regulating genes
  - Analysis of inflammation-related genes promoter PQS
  - Cell viability assay
  - Real-time quantitative polymerase chain reaction (RT-qPCR)
  - Western blot analysis
  - Enzyme-linked immunosorbent assay (ELISA)
  - Immunofluorescence analyses
  - Dot blot analysis for genomic G4
  - FCM for apoptosis detection
  - IHC evaluation
- **QUANTIFICATION AND STATISTICAL ANALYSIS**

**SUPPLEMENTAL INFORMATION**

Supplemental information can be found online at <https://doi.org/10.1016/j.isci.2022.105312>.

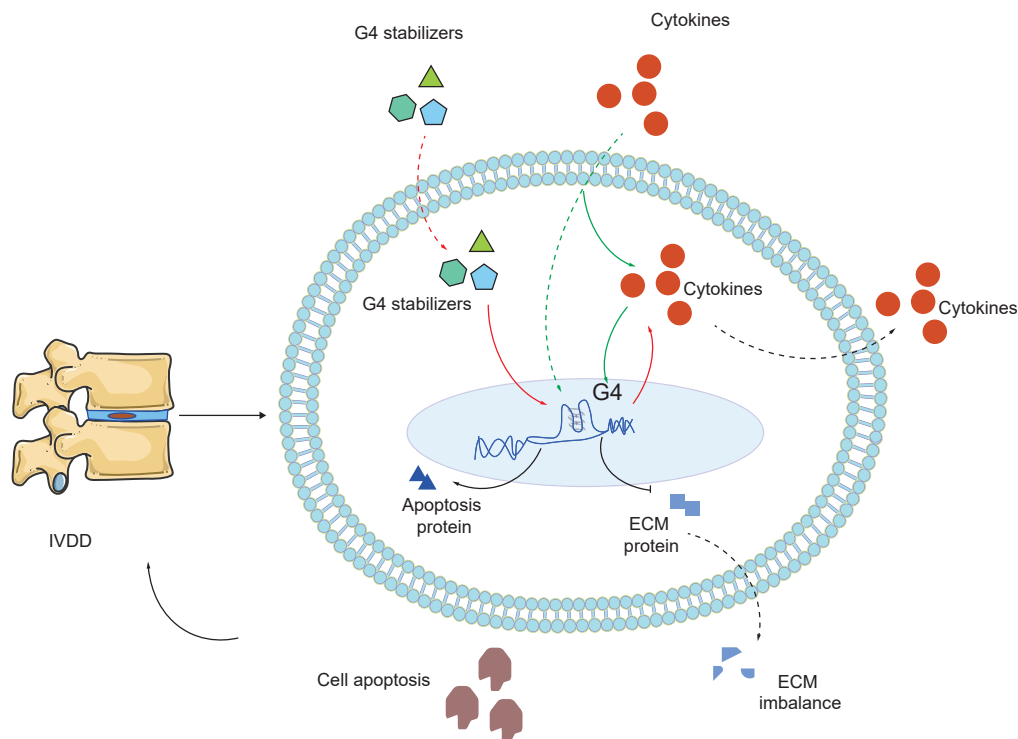


**Figure 6. Schematic illustration of the crosstalk between G4 and inflammation response in the progression of inflammation diseases**

Genomic G4 folding results in an increased inflammatory cytokines expression, and cytokines and other G4 stabilizers such as custom-made small molecules could facilitate genomic G4 folding. The progress was accompanied by cell cytokines and ECM imbalance in the IVDD mice model. G4, G-Quadruplex. ECM, extracellular matrix. IVDD, intervertebral disc degeneration.

## ACKNOWLEDGMENTS

This study was supported by the following funding: National Natural Science Foundation of China (No. 81972098, JW; No. 81902877, HY; No. 81972245, YL; No. 82173067, YL); Natural Science Foundation of Guangdong Province (2022A1515010341, JW; 2022A1515012656, HY); Science and Technology Program of Guangzhou (202201011004, HY); Excellent Talent Training Project of the Sixth Affiliated Hospital of Sun Yat-sen University (No. R2021217202512965, YL); Program of Introducing Talents of Discipline to Universities, and National Key Clinical Discipline (2012).

## AUTHOR CONTRIBUTIONS

Conceptualization: X.W., H.Y., and J.W.; Methodology: S.C., Z.Z., X.W., and H.Y.; Investigation: S.C., F.C., Y.H., and X.G.; Visualization: S.C., X.W., L.L., and W.W.; Supervision: H.Y., Y.L., and J.W.; Writing – original draft: X.W., S.C., and Z.Z.; Writing – review and editing: H.Y., J.W., and Y.L. All authors have seen and approved the final manuscript.

## DECLARATION OF INTERESTS

The authors declare that they have no competing interests.

Received: May 11, 2022

Revised: August 14, 2022

Accepted: October 5, 2022

Published: November 18, 2022



**REFERENCES**

- Beauvarlet, J., Bensadoun, P., Darbo, E., Labrunie, G., Rousseau, B., Richard, E., Draskovic, I., Londono-Vallejo, A., Dupuy, J.W., Nath Das, R., et al. (2019). Modulation of the ATM/autophagy pathway by a G-quadruplex ligand tips the balance between senescence and apoptosis in cancer cells. *Nucleic Acids Res.* 47, 2739–2756. <https://doi.org/10.1093/nar/gkz095>.
- Bedawi, M.K., Almaghlouth, I., and Omair, M.A. (2021). Effectiveness and adverse effects of anakinra in treatment of rheumatoid arthritis: a systematic review. *Eur. Rev. Med. Pharmacol. Sci.* 25, 7833–7839. [https://doi.org/10.26355/eurrev\\_202112\\_27630](https://doi.org/10.26355/eurrev_202112_27630).
- Bidula, S. (2021). Analysis of putative G-quadruplex forming sequences in inflammatory mediators and their potential as targets for treating inflammatory disorders. *Cytokine* 142, 155493. <https://doi.org/10.1016/j.cyto.2021.155493>.
- Carelli, S., Giallongo, T., Gombalova, Z., Rey, F., Gorio, M.C.F., Mazza, M., and Di Giulio, A.M. (2018). Counteracting neuroinflammation in experimental Parkinson's disease favors recovery of function: effects of Er-NPCs administration. *J. Neuroinflammation* 15, 333. <https://doi.org/10.1186/s12974-018-1375-2>.
- Chen, F., Jiang, G., Liu, H., Li, Z., Pei, Y., Wang, H., Pan, H., Cui, H., Long, J., Wang, J., and Zheng, Z. (2020). Melatonin alleviates intervertebral disc degeneration by disrupting the IL-1beta/NF-kappaB-NLRP3 inflammasome positive feedback loop. *Bone Res.* 8, 10. <https://doi.org/10.1038/s41413-020-0087-2>.
- Cruz, S.M., and Balkwill, F.R. (2015). Inflammation and cancer: advances and new agents. *Nat. Rev. Clin. Oncol.* 12, 584–596. <https://doi.org/10.1038/nrclinonc.2015.105>.
- Cubero, F.J., Woitok, M.M., Zoubek, M.E., de Bruin, A., Hatting, M., and Trautwein, C. (2019). Disruption of the FasL/Fas axis protects against inflammation-derived tumorigenesis in chronic liver disease. *Cell Death Dis.* 10, 115. <https://doi.org/10.1038/s41419-019-1391-x>.
- Dreos, R., Ambrosini, G., Périer, R.C., and Bucher, P. (2015). The Eukaryotic Promoter Database: expansion of EPDnew and new promoter analysis tools. *Nucleic Acids Res.* 43, D92–D96. <https://doi.org/10.1093/nar/gku111>.
- Enuka, Y., Feldman, M.E., Chowdhury, A., Srivastava, S., Lindzen, M., Sas-Chen, A., Massart, R., Cheishvili, D., Suderman, M.J., Zaltsman, Y., et al. (2017). Epigenetic mechanisms underlie the crosstalk between growth factors and a steroid hormone. *Nucleic Acids Res.* 45, 12681–12699. <https://doi.org/10.1093/nar/gkx865>.
- Feehan, K.T., and Gilroy, D.W. (2019). Is resolution the end of inflammation? *Trends Mol. Med.* 25, 198–214. <https://doi.org/10.1016/j.molmed.2019.01.006>.
- Guo, J.U., and Bartel, D.P. (2016). RNA G-quadruplexes are globally unfolded in eukaryotic cells and depleted in bacteria. *Science* 353, aaf5371. <https://doi.org/10.1126/science.aaf5371>.
- Hänsel-Hertsch, R., Spiegel, J., Marsico, G., Tannahill, D., and Balasubramanian, S. (2018). Genome-wide mapping of endogenous G-quadruplex DNA structures by chromatin immunoprecipitation and high-throughput sequencing. *Nat. Protoc.* 13, 551–564. <https://doi.org/10.1038/nprot.2017.150>.
- Hartvigsen, J., Hancock, M.J., Kongsted, A., Louw, Q., Ferreira, M.L., Genevay, S., Hoy, D., Karpinen, J., Pransky, G., Sieper, J., et al. (2018). What low back pain is and why we need to pay attention. *Lancet* 391, 2356–2367. [https://doi.org/10.1016/s0140-6736\(18\)30480-x](https://doi.org/10.1016/s0140-6736(18)30480-x).
- Holmes, C. (2013). Review: systemic inflammation and Alzheimer's disease. *Neuropathol. Appl. Neurobiol.* 39, 51–68. <https://doi.org/10.1111/j.1365-2990.2012.01307.x>.
- Huang, J., Li, G., Wu, Z., Song, Z., Zhou, Y., Shuai, L., Weng, X., Zhou, X., and Yang, G. (2009). Bisbenzimidazole to benzobisimidazole: from binding B-form duplex DNA to recognizing different modes of telomere G-quadruplex. *Chem. Commun.* 902–904. <https://doi.org/10.1039/b819789j>.
- Kay, J., Thadhani, E., Samson, L., and Engelward, B. (2019). Inflammation-induced DNA damage, mutations and cancer. *DNA Repair* 83, 102673. <https://doi.org/10.1016/j.dnarep.2019.102673>.
- Khandia, R., and Munjal, A. (2020). Interplay between inflammation and cancer. *Adv. Protein Chem. Struct. Biol.* 119, 199–245. <https://doi.org/10.1016/bs.apcsb.2019.09.004>.
- Koerner, J.D., Markova, D.Z., Schroeder, G.D., Rihn, J.A., Hilibrand, A.S., Vaccaro, A.R., Anderson, D.G., and Kepler, C.K. (2016). The effect of substance P on an intervertebral disc rat organ culture model. *Spine* 41, 1851–1859. <https://doi.org/10.1097/BRS.0000000000001676>.
- Kwok, C.K., and Merrick, C.J. (2017). G-quadruplexes: prediction, characterization, and biological application. *Trends Biotechnol.* 35, 997–1013. <https://doi.org/10.1016/j.tibtech.2017.06.012>.
- Lago, S., Nadai, M., Cernilogar, F.M., Kazerani, M., Domínguez Moreno, H., Schotta, G., and Richter, S.N. (2021). Promoter G-quadruplexes and transcription factors cooperate to shape the cell type-specific transcriptome. *Nat. Commun.* 12, 3885. <https://doi.org/10.1038/s41467-021-24198-2>.
- Lane, A.N., Chaires, J.B., Gray, R.D., and Trent, J.O. (2008). Stability and kinetics of G-quadruplex structures. *Nucleic Acids Res.* 36, 5482–5515. <https://doi.org/10.1093/nar/gkn517>.
- Li, C., Wang, H., Yin, Z., Fang, P., Xiao, R., Xiang, Y., Wang, W., Li, Q., Huang, B., Huang, J., and Liang, K. (2021). Ligand-induced native G-quadruplex stabilization impairs transcription initiation. *Genome Res.* 31, 1546–1560. <https://doi.org/10.1101/gr.275431.121>.
- Liu, S., Bu, L., Zhang, Y., Yan, J., Li, L., Li, G., Song, Z., and Huang, J. (2021). Subtle structural changes of dyers lead to distinctly different fluorescent behaviors in cellular context: the role of G-quadruplex DNA interaction using coumarin-quinazolinone conjugates as a case study. *Anal. Chem.* 93, 5267–5276. <https://doi.org/10.1021/acs.analchem.1c00301>.
- Long, J., Wang, X., Du, X., Pan, H., Wang, J., Li, Z., Liu, H., Li, X., and Zheng, Z. (2019). JAG2/Notch2 inhibits intervertebral disc degeneration by modulating cell proliferation, apoptosis, and extracellular matrix. *Arthritis Res. Ther.* 21, 213. <https://doi.org/10.1186/s13075-019-1990-z>.
- Love, M.I., Huber, W., and Anders, S. (2014). Moderated estimation of fold change and dispersion for RNA-seq data with DESeq2. *Genome Biol.* 15, 550. <https://doi.org/10.1186/s13059-014-0550-8>.
- Lyu, J., Shao, R., Kwong Yung, P.Y., and Elsässer, S.J. (2021). Genome-wide mapping of G-quadruplex structures with CUT&Tag. *Nucleic Acids Res.* 50, e13. <https://doi.org/10.1093/nar/gkab1073>.
- Maiti, S., Saha, P., Das, T., Bessi, I., Schwalbe, H., and Dash, J. (2018). Human telomeric G-quadruplex selective fluoro-isoquinolines induce apoptosis in cancer cells. *Bioconjug. Chem.* 29, 1141–1154. <https://doi.org/10.1021/acs.bioconjchem.7b00781>.
- Mao, S.Q., Ghanbarian, A.T., Spiegel, J., Martínez Cuesta, S., Beraldi, D., Di Antonio, M., Marsico, G., Hänsel-Hertsch, R., Tannahill, D., and Balasubramanian, S. (2018). DNA G-quadruplex structures mold the DNA methylome. *Nat. Struct. Mol. Biol.* 25, 951–957. <https://doi.org/10.1038/s41594-018-0131-8>.
- Markopoulos, G.S., Roupakia, E., Marcu, K.B., and Kolettas, E. (2019). Epigenetic regulation of inflammatory cytokine-induced epithelial-to-mesenchymal cell transition and cancer stem cell generation. *Cells* 8. <https://doi.org/10.3390/cells8101143>.
- Marsico, G., Chambers, V.S., Sahakyan, A.B., McCauley, P., Boutell, J.M., Antonio, M.D., and Balasubramanian, S. (2019). Whole genome experimental maps of DNA G-quadruplexes in multiple species. *Nucleic Acids Res.* 47, 3862–3874. <https://doi.org/10.1093/nar/gkz179>.
- Medzhitov, R. (2008). Origin and physiological roles of inflammation. *Nature* 454, 428–435. <https://doi.org/10.1038/nature07201>.
- Priyadarshani, P., Li, Y., and Yao, L. (2016). Advances in biological therapy for nucleus pulposus regeneration. *Osteoarthritis Cartilage* 24, 206–212. <https://doi.org/10.1016/j.joca.2015.08.014>.
- Risbud, M.V., and Shapiro, I.M. (2014). Role of cytokines in intervertebral disc degeneration: pain and disc content. *Nat. Rev. Rheumatol.* 10, 44–56. <https://doi.org/10.1038/nrrheum.2013.160>.
- Robinson, W.H., Lepus, C.M., Wang, Q., Raghu, H., Mao, R., Lindstrom, T.M., and Sokolove, J. (2016). Low-grade inflammation as a key mediator of the pathogenesis of osteoarthritis. *Nat. Rev. Rheumatol.* 12, 580–592. <https://doi.org/10.1038/nrrheum.2016.136>.
- Sengupta, A., Roy, S.S., and Chowdhury, S. (2021). Non-duplex G-quadruplex DNA structure: a developing story from predicted sequences to

DNA structure-dependent epigenetics and beyond. *Acc. Chem. Res.* 54, 46–56. <https://doi.org/10.1021/acs.accounts.0c00431>.

Sen, D., and Gilbert, W. (1988). Formation of parallel four-stranded complexes by guanine-rich motifs in DNA and its implications for meiosis. *Nature* 334, 364–366.

Steven, S., Frenis, K., Oelze, M., Kalinovic, S., Kuntic, M., Bayo Jimenez, M.T., Vujacic-Mirski, K., Helmstädter, J., Kröller-Schön, S., Münzel, T., and Daiber, A. (2019). Vascular inflammation and oxidative stress: major triggers for cardiovascular disease. *Oxid. Med. Cell. Longev.* 2019, 7092151. <https://doi.org/10.1155/2019/7092151>.

Strowig, T., Henao-Mejia, J., Elinav, E., and Flavell, R. (2012). Inflammasomes in health and disease. *Nature* 481, 278–286. <https://doi.org/10.1038/nature10759>.

Sun, X., Yu, J., Wong, S.H., Chan, M.T.V., Zhang, L., and Wu, W.K.K. (2022). SARS-CoV-2 targets the lysosome to mediate airway inflammatory cell death. *Autophagy* 18, 2246–2248. <https://doi.org/10.1080/15548627.2021.2021496>.

Tarnowski, M., Kopytko, P., and Piotrowska, K. (2021). Epigenetic regulation of inflammatory responses in the context of physical activity. *Genes* 12, 1313. <https://doi.org/10.3390/genes12091313>.

Tian, T., Chen, Y.-Q., Wang, S.-R., and Zhou, X. (2018). G-quadruplex: a regulator of gene

expression and its chemical targeting. *Chem* 4, 1314–1344. <https://doi.org/10.1016/j.chempr.2018.02.014>.

Varshney, D., Spiegel, J., Zyner, K., Tannahill, D., and Balasubramanian, S. (2020). The regulation and functions of DNA and RNA G-quadruplexes. *Nat. Rev. Mol. Cell Biol.* 21, 459–474. <https://doi.org/10.1038/s41580-020-0236-x>.

Verma, A., Halder, K., Halder, R., Yadav, V.K., Rawal, P., Thakur, R.K., Mohd, F., Sharma, A., and Chowdhury, S. (2008). Genome-wide computational and expression analyses reveal G-quadruplex DNA motifs as conserved cis-regulatory elements in human and related species. *J. Med. Chem.* 51, 5641–5649.

Vergoesen, P.P.A., Kingma, I., Emanuel, K.S., Hoogendoorn, R.J.W., Welting, T.J., van Royen, B.J., van Dieën, J.H., and Smit, T.H. (2015). Mechanics and biology in intervertebral disc degeneration: a vicious circle. *Osteoarthritis Cartilage* 23, 1057–1070. <https://doi.org/10.1016/j.joca.2015.03.028>.

Wang, J., Tian, Y., Phillips, K.L.E., Chiverton, N., Haddock, G., Bunning, R.A., Cross, A.K., Shapiro, I.M., Le Maitre, C.L., and Risbud, M.V. (2013). Tumor necrosis factor alpha- and interleukin-1beta-dependent induction of CCL3 expression by nucleus pulposus cells promotes macrophage migration through CCR1. *Arthritis Rheum.* 65, 832–842. <https://doi.org/10.1002/art.37819>.

Wang, R.P., Leung, W., Goto, T., Ho, J.Y., and Chang, R.C. (2021). IL-1 beta and TNF-alpha play an essential role in modulating the risk of both periodontitis and Alzheimer's disease. *Alzheimer's Dementia* 17 (Suppl 12), e058464. <https://doi.org/10.1002/alz.058464>.

Wang, Y., Che, M., Xin, J., Zheng, Z., Li, J., and Zhang, S. (2020). The role of IL-1beta and TNF-alpha in intervertebral disc degeneration. *Biomed.Pharmacother.* 131, 110660. <https://doi.org/10.1016/j.biopha.2020.110660>.

Wenzel, P., Kossmann, S., Münzel, T., and Daiber, A. (2017). Redox regulation of cardiovascular inflammation - immunomodulatory function of mitochondrial and Nox-derived reactive oxygen and nitrogen species. *Free Radic. Biol. Med.* 109, 48–60. <https://doi.org/10.1016/j.freeradbiomed.2017.01.027>.

Zhang, R., Lin, Y., and Zhang, C.T. (2008). Greglist: a database listing potential G-quadruplex regulated genes. *Nucleic Acids Res.* 36, D372–D376. <https://doi.org/10.1093/nar/gkm787>.

Zimmer, J., Tacconi, E.M.C., Folio, C., Badie, S., Porru, M., Klare, K., Tumiati, M., Markkanen, E., Halder, S., Ryan, A., et al. (2016). Targeting BRCA1 and BRCA2 deficiencies with G-quadruplex-interacting compounds. *Mol. Cell* 61, 449–460. <https://doi.org/10.1016/j.molcel.2015.12.004>.



## STAR★METHODS

### KEY RESOURCES TABLE

REAGENT or RESOURCE	SOURCE	IDENTIFIER
<b>Antibodies</b>		
anti-1H6	Millipore	Cat#MABE1126; RRID:AB_2924428
anti-BG4	Millipore	Cat#MABE917; RRID:AB_2750936
anti-TNF- $\alpha$	BioVision	Cat#3052R-100; RRID:AB_2203941
anti-IL-6	Zen BioScience	Cat#500286; RRID:AB_2924431
anti-aggrecan	Abcam	Cat#ab3778; RRID:AB_304071
anti-collagen II	Abcam	Cat#ab34712; RRID:AB_731688
anti-cleaved caspase-3	Zen BioScience	Cat#341034; RRID:AB_2924432
anti-Bcl-2	Zen BioScience	Cat#381702; RRID:AB_2924433
anti-Bax	Zen BioScience	Cat#380709; RRID:AB_2924434
<b>Biological samples</b>		
Sprague–Dawley rats	Laboratory Animal Center of Sun Yat-Sen University	N/A
C57BL/6 mice	GemPharmatech Co., Ltd.	N/A
<b>Chemicals, peptides, and recombinant proteins</b>		
Recombinant human TNF- $\alpha$	Peprotech	Cat#300-01A
Recombinant human IL-1 $\beta$	Peprotech	Cat#200-01B
Recombinant human IL-6	Peprotech	Cat#200-06
Pyridostatin (PDS)	MedChemExpress	Cat#551487
Braco-19	MedChemExpress	Cat#555687
Phen-DC3	MedChemExpress	Cat#562479
Cell Counting Kit	APExBIO	Cat#K1018-500T
SYBR Green Mix	Roche	Cat#4713860
ELISA kits	MultiSciences	Cat#EK382HS-96; Cat#EK301B/3-96; Cat#EK306/3-96
Annexin V-FITC_P1 apoptosis kit	MultiSciences	Cat#70-AP101-100
<b>Deposited data</b>		
RNA-seq	GEO	GSE194015
<b>Oligonucleotides</b>		
$\beta$ -actin	Tianyi Huiyuan	F 5'-ATCATTGCTCCTCCTGAGCG-3' R 5'-AGCTCAGTAACAGTCCGCC-3'
Tnfa	Tianyi Huiyuan	F 5'-GATCGGTCCCAACAAGGAGG-3' R 5'-GCTTGGTGGTTTGCTACGAC-3'
Il1b	Tianyi Huiyuan	F 5'-GACTTCACCATGGAACCCGT-3' R 5'-CAGGGAGGGAAACACCGTT-3'
Il6	Tianyi Huiyuan	F 5'-ACAAGTCCGGAGAGGAGACT-3' R 5'-ACAGTGCATCATCGTGTT-3'
<b>Software and algorithms</b>		
GraphPad Prism 7	GraphPad Software	N/A
FlowJo_V10	FlowJo Software	N/A
R (4.1.2)	The R foundation	<a href="https://www.r-project.org/">https://www.r-project.org/</a>
RStudio	RStudio Team	<a href="https://www.rstudio.com/">https://www.rstudio.com/</a>

(Continued on next page)

**Continued**

REAGENT or RESOURCE	SOURCE	IDENTIFIER
DESeq2	R-Bioconductor	<a href="https://bioconductor.org/packages/release/bioc/html/DESeq2.html">https://bioconductor.org/packages/release/bioc/html/DESeq2.html</a>
clusterProfiler	R-Bioconductor	<a href="https://bioconductor.org/packages/release/bioc/html/clusterProfiler.html">https://bioconductor.org/packages/release/bioc/html/clusterProfiler.html</a>
QGRS Mapper	<a href="https://doi.org/10.1093/nar/gkl253">https://doi.org/10.1093/nar/gkl253</a>	<a href="https://bioinformatics.ramapo.edu/QGRS/index.php">https://bioinformatics.ramapo.edu/QGRS/index.php</a>
G4 Hunter	<a href="https://doi.org/10.1093/nar/gkw006">https://doi.org/10.1093/nar/gkw006</a>	<a href="https://bioinformatics.ibp.cz/#/analyse/quadruplex">https://bioinformatics.ibp.cz/#/analyse/quadruplex</a>

**RESOURCE AVAILABILITY****Lead contact**

Further information and requests for resources and reagents should be directed to and will be fulfilled by the lead contact, Jianru Wang ([wangjru@mail.sysu.edu.cn](mailto:wangjru@mail.sysu.edu.cn))

**Materials availability**

This study did not generate new unique reagents.

**Data and code availability**

Any additional information required to reanalyze the data reported in this article is available from the [lead contact](#) on request. The RNA-seq profiles have been deposited on GEO with the identifier of GSE194015. The datasets used and analyzed in the current study are available from the corresponding author on reasonable request.

**EXPERIMENTAL MODEL AND SUBJECT DETAILS****Isolation and culture of primary rat NP cells**

The mature male Sprague–Dawley rats aged at 6 weeks and weighing 200–300g were obtained from the Laboratory Animal Center of Sun Yat-sen University, China. Rat NP cells were isolated from the lumbar discs of Sprague–Dawley rats and cultured *in vitro* (Long et al., 2019). The details of the procedure are as follows. After being euthanized using pentobarbital sodium (100 mg/kg), The spinal columns of Sprague–Dawley rats were removed and discs were separated. The NP tissues were cut into pieces, digested, and then cultured in DMEM (Invitrogen, CA, USA) containing 10% fetal bovine serum and 2% penicillin-streptomycin antibiotics at 37°C in a humidified incubator with 5% CO<sub>2</sub>. About 7 days later, the NP cells migrated out and cells were passaged using trypsin. NP cells within 3–7 generations were used in this study.

**Animal model and MRI**

We constructed the IVDD animal model with AF needle puncture using WT C57BL/6 mice (Chen et al., 2020). Male C57BL/6 mice were obtained from GemPharmatech Co., Ltd. In brief, after anesthesia and a small longitudinal incision of the abdominal wall was performed in the supine posture, we found the L4/5 intervertebral disc at the level of renal vein. Thirty mice were randomly divided into six groups (5 mice per group), including the normal group not operated, the IVDD group, the sham group injected with 0.9% normal saline using a syringe needle through AF, the PDS group injected with PDS, the Braco-19 group injected with Braco-19. After the L4/5 IVD was exposed under a microscope, the discs were punctured and injected with 2μL PBS, G4 stabilizers by a 31G syringe needle inserted 1.5 mm into the discs, respectively. At 4 weeks after surgery, all mice underwent MRI scans under anesthesia, and the T2 mapping MRI sequence was used to evaluate the degree of IVDD.

**Ethical approval**

The study protocol was reviewed and approved by the Institutional Review Board of Sun Yat-sen University. The animal experiments were approved by the Animal Experimentation Committee of Medical Ethics Committee of The Sixth Affiliated Hospital of Sun Yat-sen University (IACUC-2020120102).

## METHOD DETAILS

### RNA-seq analysis for potential G4-regulating genes

We used the 'DESeq2' R package to identify DEGs (Love et al., 2014). The genes with FDR of 0.05 and absolute fold change of 1.5 in the DEG analysis were obtained for downstream analysis. The algorithm-predicted PQS of *Rattus norvegicus* was obtained from an online database (<http://tubic.tju.edu.cn/greglist>) (Zhang et al., 2008). PQS is the motif featured by G3+N1–7G3+N1–7G3+N1–7G3+ (Zhang et al., 2008). A total of 7,013 genes were predicted to contain PQS in *Rattus norvegicus*. By analyzing the G4-stabilization-specific DEGs and algorithm-predicted PQS, we identified and defined the PQRGs. We used the 'cluster profile' R package to perform the GO enrichment and KEGG enrichment analysis for PQRGs.

### Analysis of inflammation-related genes promoter PQS

A total of 96 inflammation related genes were collected from prior research (Bidula, 2021) and their orthologous *Rattus norvegicus* genes were used in the current study. By analyzing the algorithm-predicted PQS and inflammation-related genes, we identified 23 potential G4-regulating inflammation-related genes. The distribution of PQS within different genomic regions was analyzed. Promoter regions of inflammation-related PQRGs were obtained from an online database (Eukaryotic Promoter Database, EPD, <http://epd.vital-it.ch>) (Dreos et al., 2015), and the genomic regions from –900 to +300 base pairs concerning the transcription start site were retrieved.

### Cell viability assay

NP cells viability was examined following exposure to small molecular compounds for 0, 12, 24, 36, 48, or 72 h, and counted using a Cell Counting Kit (CCK-8) as the manufacturer's protocol. Using a microplate reader (Thermo Fisher Scientific), we assessed cell viability through absorbance detection at 450 nm. According to treatment, NP cells were segmented into four groups, control (DMSO only), PDS treated, Braco-19 treated, and Phen-DC3 treated groups and every group was divided into different subgroups by doses. Cells were seeded in 96-well culture plates at the density of  $1 \times 10^3$  per well with 100  $\mu$ L of complete culture medium. The cells were then cultured for another 12, 24, 36, 48, and 72 h treated with G4 stabilizers after 24 h. 10  $\mu$ L CCK-8 solution was applied at specific time points, then cells were incubated in the dark for 2-4 h at 37°C.

### Real-time quantitative polymerase chain reaction (RT-qPCR)

Total RNA was isolated with cells using a reagent, and cDNA was reversed as directed by the manufacturer. RT-qPCR was performed using SYBR Green PCR Kit and was run on QuantStudio 5 Real-Time PCR System (Thermo Fisher Scientific). All primers were synthesized by Tianyi Huiyuan Biotech Co., Ltd. Total RNA was isolated with cells using a reagent, and cDNA was reversed as directed by the manufacturer. RT-qPCR was performed using SYBR Green PCR Kit and was run on QuantStudio 7 Real-Time PCR System (Thermo Fisher Scientific).  $\beta$ -actin was used to normalize the expression levels of target genes. All primers were synthesized by Tianyi Huiyuan Biotech Co., Ltd. The oligos used in the RT-qPCR assays were as follows:  $\beta$ -actin F 5'-ATCATTGCTCCTCTGAGCG-3', R 5'-AGCTCAGTAACAGTCCGCC-3'; Tnfa F 5'-GATCGGTCCCAACAA GGAGG-3', R 5'-GCTTGGTGGTTTGCTACGAC-3'; Il1b F 5'-GACTTCACCATGGAACCCGT-3', R 5'-CA GGGAGGGAAACACACGTT-3'; Il6 F 5'-ACAAGTCCGGAGAGGAGACT-3', R 5'-ACAGTGCATCATCG CTGTTC-3'. RT-qPCR analysis was carried out with a cycle setup of 3minat 95°C, 40 cycles of 5sat 95°C and 20sat 60°C.

### Western blot analysis

The proteins from extracted cell lysates were separated by SDS-PAGE gel electrophoresis followed by transfer and immunoblotting (Chen et al., 2020). The process was as follows. The protein was extracted and the concentration was measured by a BCA Kit (Pierce Biotechnology, Rockford, IL, USA). After electroblotting, the membranes were blocked in 5% skim milk powder and incubated with primary antibodies targeting cleaved-caspase3, Bax, and  $\beta$ -actin. After washing with PBS, the membranes were incubated with HRP-linked anti-rabbit immunoglobulin G (IgG; 1:1000, Cell Signaling Technology) or HRP-linked anti-mouse IgG (1:1000, Cell Signaling Technology). Finally, the Western blot bands were tested.

### Enzyme-linked immunosorbent assay (ELISA)

NP cells grown up to confluence were treated with G4 stabilizers or cytokines for 24 h. Cell supernatants were collected and analyzed for TNF- $\alpha$  and IL-6 using specific ELISA kits (MultiSciences, EK382HS-96, EK301B/3-96, EK306/3-96) according to the manufacturer's protocol.

### Immunofluorescence analyses

NP cells were fixed for 15 min with formalin and permeabilized for 10 min with Triton X-100, followed by blocking for 1 h with 10% goat serum. Cells were then incubated with G4 antibody 1H6 (1:200) and a second antibody DAPI was used to stain the nuclei of the cells. As the manufacturer's introduction, the fluorescence was captured by a confocal laser scanning microscopy (Leica).

### Dot blot analysis for genomic G4

G4 stabilizers or cytokines were used to treat NP cells. Then, they were cross-linked in 1% formalin for 10 min at 37°C and stopped by 125 mM glycine solution for 5 min. Next, washed NP cells were lysed for protein extraction. Samples were divided into two 50  $\mu$ L parts separately. One was collected and saved at  $-80^{\circ}\text{C}$  for dot blot analysis, and the other one was carried out for quantitation and normalized relative to the control group. Subsequently, each sample was diluted into 100 ng/ $\mu$ L in intracellular salt solution (25 mM HEPES pH 7.5, 10.5 mM NaCl, 110 mM KCl, 130 nM  $\text{CaCl}_2$ , 1 mM  $\text{MgCl}_2$ ). 5  $\mu$ L different nucleic acid samples were pipetted and dotted on a nylon membrane. Membranes were dried in the air and nucleic acids were immobilized to the membrane for 5 to 15 min by UV light (254 nm) cross-linking at room temperature (RT). Next, the membrane was incubated for 2 h at RT or overnight at  $4^{\circ}\text{C}$  in G4 blocking buffer (1% BSA in an intracellular salt solution) and washed with G4 washing buffer (10 mM Tris pH 7.4, 100 mM KCl, 0.1% (v/v) Tween 20) three times. After that, these membranes were incubated with G4 structure antibodies BG4 (1:500 in G4 blocking buffer) overnight at  $-4^{\circ}\text{C}$ . After washing three times by G4 washing buffer, the membranes (1:1000 in G4 blocking buffer) were incubated with secondary antibodies and visualized by an ECL system like Western blot analysis.

### FCM for apoptosis detection

Apoptosis was evaluated by staining cultured primary NP cells with both FITC and PI according to the manufacturer's introduction (MultiSciences, 70-AP101-100) and then analyzed with FCM (Beckman Coulter, CA, USA).

### IHC evaluation

After MRI scanning, the spines were removed and fixed with 4% (w/v) paraformaldehyde, followed by decalcification in EDTA solution. According to the standard procedures, the histological slides were deparaffinized and rehydrated, followed by staining with hematoxylin and eosin (H&E), Safranin O-Fast Green. IHC was performed as we described previously (Chen et al., 2020). Briefly, anti-G4 (1H6, 1:200), anti-aggrecan, anti-collagen II, and anti-MMP3 were used to incubate sections overnight at  $4^{\circ}\text{C}$  and then incubated with a secondary antibody. Nuclear was under staining by hematoxylin. Finally, a slides canner was performed to observe and capture digital photos of these samples. The histologic scores were evaluated from five categories of IVDD changes, including the cellularity, morphology and border between AF and NP, and a scale with scores ranging from 5 points (a normal disc) to 15 points (a severely degenerated disc) was used.

### QUANTIFICATION AND STATISTICAL ANALYSIS

Statistical analyses were performed with GraphPad Prism statistical software (GraphPad Software Inc) and R software (R Core Team). The two-sided Student's t-test was used for comparing two groups and the one-way ANOVA test was used for comparing 3 or more groups. Significance was considered for  $p < 0.05$ . Data were represented as mean (SEM).